(Received 31 May 2025, Accepted 11 July 2025, Scheduled 4 August 2025)

Adding of Metacell Units for Efficient Performance of Circular Patch Antenna

Rusul M. Hashim and Mohammed T. Gatte*

Department of Electrical Engineering, College of Engineering, University of Babylon, Iraq

ABSTRACT: This work is motivated by the recently domination of mobile and wireless communications technologies, in addition to the fast evolution of the new generation of mobile and wireless communication that leads to the successive mobile generations XG 3G, 4G, 5G, and in near future 6G. Currently, the fifth generation (5G) technologies still need more development for a compact and efficient device. In this manuscript, Meta cells units (metamaterial and metasurface) are employed for improving the main parameters of antenna performance like gain (G), bandwidth (BW), reflection coefficient (S_{11}), and radiation efficiency. The proposed antenna design shows multiple resonant frequencies which means that the design is able to operate at multiband of frequencies, including 6 GHz band that considers the main targeted band of 4G and 5G mobile communication technologies. The simulation results, for the different models via adding meta cells to the proposed design model, show excellent improvement for the performance parameters that are improved excellently in comparison with the conventional circular patch (CCP) and previous literature. In addition, the use of meta cells reduced the resonant frequency which means that it can serve a lower frequency with small size of substrate, and it is half size of CCP, making it suitable for many applications that require a compact antenna design.

1. INTRODUCTION

The currently development of wireless communications (WC), besides their recent many applications, which lead the researchers to concentrate their attention on the study and development of this topic that has great impact, in the life system, makes it involve in different fields like medical space communication engineering. There is need for the device's improvement used in the field of communications and developing them to suit the current and future generations of mobile communications [1]. Antennas are considered the main part of WC which should be developed to match the requirement of the current and next generation of WC (4G, 5G, and 6G). Moreover, parameters such as low power consumption, higher gain, bandwidth, and radiation efficiency are targeted to get efficient antenna and WC system [2–4]. These parameters are significant for the improvement of channel capacity, which is important to enhancing speed and security to achieve high data rate and secure communication. The design of an efficient antenna not only depends on the investigation of antennas engineers, but also requires the participation of physicists and materials scientists [5]. Many researchers suggest the use of nanomaterials for the improvement of antenna behaviour and performance parameters [6, 7]. Nanomaterials, such as graphene and carbon nanotube, are utilized in different techniques like coating and metamaterials for the enhancement of antenna performance [8, 9]. Since it was invented more than fifty years ago, metamaterial technique has attracted the attention of many researchers, to use it in the enhancement of antenna performance parameters [10, 11]. Metamaterials do not exist in nature, and they are artificially designed and fabricated via removing part(s) as a slot from the conducting layer of patch or plane or adding a parasitic element as SRR depending on an optimized process [12], where the conventional material (such as copper of the conducting layer) is designed in a specific geometric shape that leads to different electrical and magnetic properties that do not exist in nature, like permittivity and negative permeability, and this technique is useful for achieving a small structural size, high gain, and high frequency range [13]. Metamaterials emerge as a promising technology to overcome design challenges by tuning the unit cell properties of metamaterials using techniques such as split ring resonators (SRRs) by adjusting their geometric parameters. Metamaterials are one of the techniques used in the improvement of antennas design [14], where the parasitic elements create an additional coupling path to oppose the signal from the other path, electromagnetic band gap (EBG) [13], split ring resonators (SRRs) [15]. Many designs have limitations such as large size, narrow bandwidth (NBW), or operation outside of 5G bands [10]. In this work, metamaterials have also been used to provide improvement for the circular patch antenna performance parameters, and the effect of this technique on the antenna behaviour at multiple resonances of 5G bands leads to an improvement in gain, bandwidth and radiation efficiency [16]. This paper is extended to the work in [17] , where it comes in four sections, the second section presents the design methodology, while the third section illustrates the results and dissection, and fourth section explains the main conclusions of this work.

* Corresponding author: Mohammed Taih Gatte (mohammed.taih@uobabylon.edu.iq).

2. MATERIALS AND METHODS

2.1. Metamaterial

The proposed antenna design basically depends on a circular patch, which represents an approach that considers the origin (base) model M00. The computer simulation software CST is used in the design of the proposed antenna model. The suggested shape, for the design of patch antenna, is implemented on a composite conductive layer attached to a dielectric substrate. The material of the substrate layer is FR-4, which is a square shape of $W = L = 75$ mm, with thickness $h = 1$ mm, and dielectric constant 4.3. The conventional design of a circular patch antenna is firstly used, which consists of three layers: the radiation part (patch), which is a conductor layer on the top of the antenna substrate (dielectric layer) and the ground layer which is also conducting layer at the bottom of antenna substrate, where the insulating layer will be sandwiched between the two conducting layers, the radiation and ground layers of antenna. The model is presented in Figure 1. The dimensions of the design parameters are shown in Table 1, which represents a circular patch antenna.

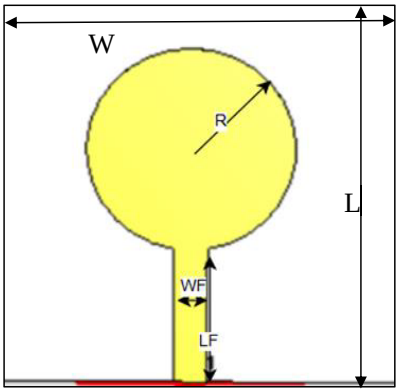

FIGURE 1. The conventional circular patch (CCP) antenna M00.

TABLE 1. The design parameters (dimensions) of the circular patch antenna M00.

The symbol	Dimensions in (mm)
W	75
L	75
WF	6
R	18.75
LF	26.78571429
T	1

Then, M00 is modified via removing a circular slot from the circular patch, and the resulting shape of the patch is an open ring, which represents an annular ring antenna. After that, two split ring resonators (SRRs) were added inside and outside the main annular ring antenna as a meta unit cell, and the inner cell has a gap from the top and the outer ring gap from the bottom. The first resulting model is considered M01, as shown in Figure 2, and Table 2 displays the dimensions of these SRRs.

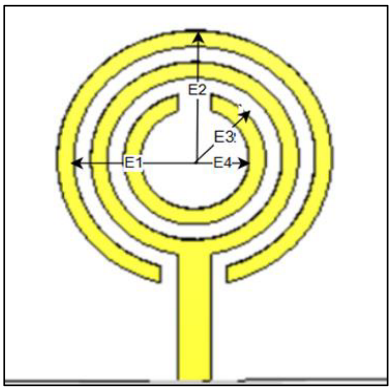

FIGURE 2. The annular patch model M01 with SRR added.

TABLE 2. The diameters of meta cells (SRR) for antenna model M01.

The symbol	Dimensions in (mm)
$E1$	21.75
$E2$	24.75
$E3$	12.75
$E4$	9.75

The second resulting model considers M02, which is modified from M01, via adoption of the same design of M01, but instead both SRRs are added inside the annular ring antenna patch, which will surround both meta cells (rings), and both of them have a small gap in the opposite direction to each other. The design of M02 is illustrated in Figure 3, and Table 3 presents its dimensions.

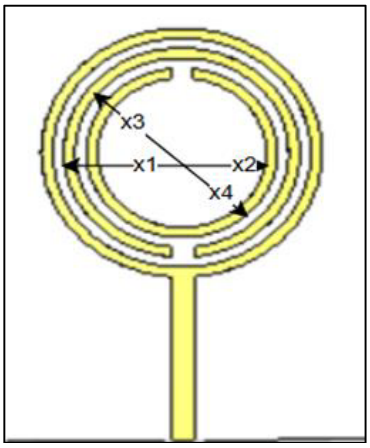

FIGURE 3. The annular patch with SRRs model M02.

The results of the three models were presented to check whether they were suitable to work at the targeted frequency and had good performance parameters, bandwidth, gain, radiation efficiency, and return loss. M00 had a bandwidth of (6.4278 to 6.6274), and the resonance occurred at 6.5076 GHz, while $S_{11} = -19.921$, while for M01, the resonance occurred at 6.4127 and $S_{11} = -24.504$. The bandwidth is (6.3303 to 6.4641), and for M02, its bandwidth is (7.5412 to 7.763). The

TABLE 3. The dimensions of the circular patch antenna model M02.

The symbol	Dimensions in (mm)
W	60
L	60
WF	2.4
$X1$	12.6
$X3$	11.4
LF	10
T	1
$X2$	9
$X4$	10.2
LF	10

resonant frequency $= 7.641$ GHz, $S_{11} = -13.795$ dB. In spite of acceptable results of these models, the performance parameters still need more improvement, to meet the requirement of an efficient antenna that can be used in 5G band of frequency, the reason that leads to follow another approach in this paper. In the second approach for the design of the first model M10, the proposed design of this model is placed on a single conducting layer substrate, where the conductive layer includes two elements, the patch (radiating element) and ground of the microstrip antenna. The proposed antenna design is placed on the conductive layer via designing and modifying the ground and radiating elements to suit the antenna design and operate at the specified frequency (resonant frequency). 6 GHz range is the targeted frequency for the proposed designs. in addition, coplanar wave (CPW) feeding is used for feeding the proposed circular patch antenna, which represents model M10 that is shown in Figure 4. The use of CPW feeding increases recently due to its advantages, compared with strip line feeding, such as low radiation loss and dispersion that makes it suitable for single conducting layer antenna [18, 19]. Model M10 was designed on a rectangular substrate, with the ground and patch placed on the same conductive copper layer. The dimensions of the design parameters are presented in Table 4. The radius of the circular patch was calculated based on the following equation [20].

TABLE 4. The dimensions of the circular patch antenna model M10.

The symbol	Dimensions in (mm)
LG	21.1
$Lg1$	10
Wg	13.2
$Wg1$	5.6
$R2$	7.35
$R5$	4.375
$R1$	R
$R4$	3.675
$R2$	7.35

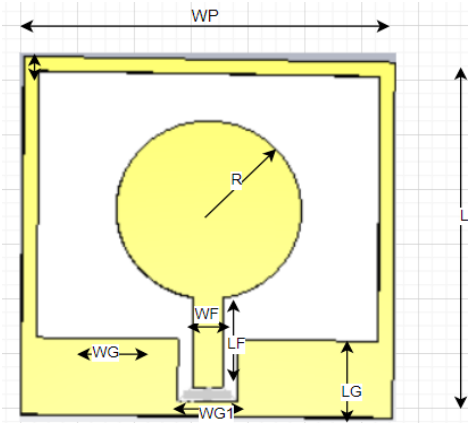

FIGURE 4. The circular patch model M10.

$$a = \frac{F}{\{1 + \frac{2h}{\pi\epsilon_r F}[\ln(\frac{\pi F}{2h}) + 1.7726]\}^{1/2}} \quad (1)$$

$$F = \frac{8.791 \times 10^9}{f_r\sqrt{\epsilon_r}} \quad (2)$$

where a: the actual radius; F: The force or constant; h: height of the substrate; f_r: resonant frequency; ϵ_r: dielectric constant of the substrate.

The antenna model M10 has been designed to operate at 6 GHz, then the model operates at the frequency resonant 6.3185 GHz with bandwidth range 5.4301 to 9.8157 GHz while $S_{11} = -23.285$ dB and gain is 5.520 dBi. Then, a circular slot is removed from the circular patch, which leads to an annular ring patch antenna, the resulting model considered M11. After that, SRRs (meta cells) are added to improve the performance of the proposed design, which is illustrated in Figure 5 that presents the model M11. Table 5 presents the dimension of design parameters for M11 based on the same dimension of M10 parameters, which leads to the following results: f_r is $= 8.4618$ GHz, and bandwidth range is 7.0973 to 9.5618 GHz while S_{11} is -17.946 dB, and gain is 4.564 dBi, which seem worse than that of M10, but the resulting circular slot in M11 makes adding of SRR easy and effective. The addition of SRR inside the annular ring patch as a meta cell (metamaterial technique) was suggested to enhance the performance of antenna = M12. Figure 6 displays the following results: $f_r = 8.3007$ GHz and bandwidth range 6.1249 to 9.3875 GHz while $S_{11} = -18.531$ dB, and gain is 5.146 dBi.

TABLE 5. The diameters of annular patch antenna M11.

The symbol	Dimensions in (mm)
R (out)	6
R (in)	5

Antenna model M12 is a developed model from model M11 via adding SRR inside the ring of this model, and Table 6 presents the dimensions of the added SRR (meta cell). After that, the design has been improved to M13 via adding another meta unit cell to the design of antenna. The dimensions of this

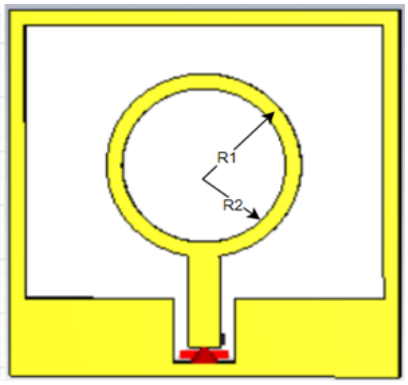

FIGURE 5. The annular ring model M11.

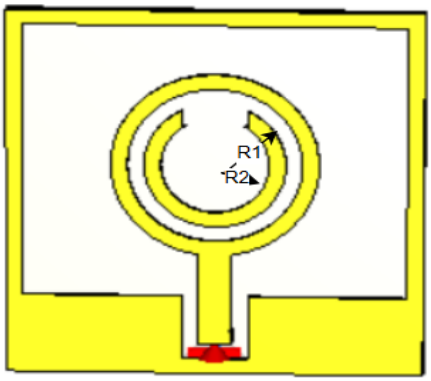

FIGURE 6. The addition of meta cell (SRR) inside the annular patch model M12.

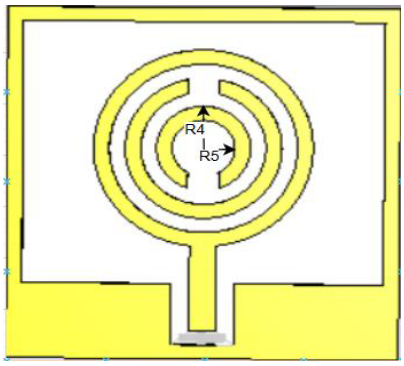

FIGURE 7. The model M13, which is an improvement of the two previous models.

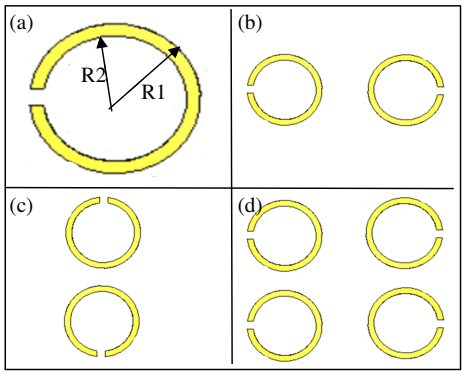

FIGURE 8. The design steps of adding meta cell on the back surface of proposed antenna designations.

TABLE 6. The diameters of the added meta cell inside the annular patch antenna M12.

The symbol	Dimensions in (mm)
$R1$ (out)	5.95
$R2$ (in)	4.55

TABLE 7. The diameter of the added meta cell to the annular patch antenna M13.

The symbol	Dimensions in (mm)
$R4$ (out)	4.2
$R5$ (in)	2.8

meta cell are listed in Table 7, and Figure 7 illustrates the resulting design.

The new model has the following results: f_r is 8.2251 GHz, and bandwidth range is 7.5587 to 10.937 GHz while S_{11} is -24.989 dB, and gain is 5.147 dBi.

2.2. Metasurface

The meta-unit cell (SRR) is added to the proposed antenna design models. The toroidal unit cell was used to improve the performance of the previous four models (circular patch antennas M10, M11, M12, and M13). The unit cell was printed on the back surface of the substrate. Three design steps were followed to add the ring(s) as a parasitic element on the back surface of the antenna substrate. In the first step, a parasitic unit cell (ring) was added on the centre of the back surface of the substrate of antenna design for the models (M20, M21, M22, M23), shown in Figure 8(a). Then in the second step, two rings were added on the back of the substrate vertically (M30, M31, M32, M33), which is illustrated in Figures 8(c) and (b) horizontally for models (M40, M41, M42, M43), while in the third step, four toroidal rings were added on the back surface of the proposed antennas (M50, M51, M52, M53) as presented in Figure 8(d). It is important to note that the measurement of the radii of the meta-surface layer is mentioned in Table 1.

3. RESULTS AND DISCUSSION

In this section, the results of the previous models are displayed and compared somewhat in stages. Firstly, the results of the models (M00, M01, and M02) are displayed in Figure 9 and Table 8. Secondly, the results of the following models (M10, M11, M12, and M13) are presented in Table 9, and Figure 10 shows the relation between frequency and return loss (S_{11}). After that, the comparison between the two groups is made for the same chosen parameters and moreover the second group that has been subjected to studying the effect of metasurface ele-

TABLE 8. The results for three model based on M00.

No	f_r GHz	S_{11} dB	BW GHz	G dBi	η %
M00	4.2	−20.74	0.14	0.34	45.10
	6.5	−19.92	0.25	3.92	22.99
	8.4	−39.55	0.268	4.8	30.29
M01	2.50	−12.53	N.W	−5.0	10.31
	6.41	−24.37	0.1	0.9	20.62
	7.60	−22.20	0.19	0.11	17.99
	8.33	−23.03	0.24	2.43	37.34
M02	5.30	−17.41	0.3	−8.7	3.02
	6.5	−14.31	0.26	−5.7	4.62
	7.7	−36.04	0.30	−4.0	5.11

TABLE 9. The results for three Model based on M10.

No	f_r GHz	S_{11} dB	BW GHz	G dBi	η %
M10	4.02	−12.87	1.57	3.45	96.87
	6.77	−21.3	4.32	5.9	94.71
M11	2.7	−11.60	0.4	2.74	95.69
	8.2	−19.0	1.610	4.3	88.12
M12	6.0	−16.19	3.5	4.0	91.48
	10.60	−47.1	0.77	5.21	79.32
M13	3.9	−19.3	0.5	2.89	91.33
	5.6	−39.03	1.66	4.6	92.89

ment on the proposed design. In the first three models, the relationship between the frequency and return loss is displayed in Figure 11, and the other parameters of antenna performance for these models are presented in Table 10.

Figure 9 and Table 8 show the poor improvement in the calculated results for these models particularly in terms of gain, radiation efficiency, and bandwidth that should be improved for these models. Then, the results for the second set of the proposed models are presented and discussed, the four models of microstrip antennas M10, M11, M12, and M13. Table 9 shows

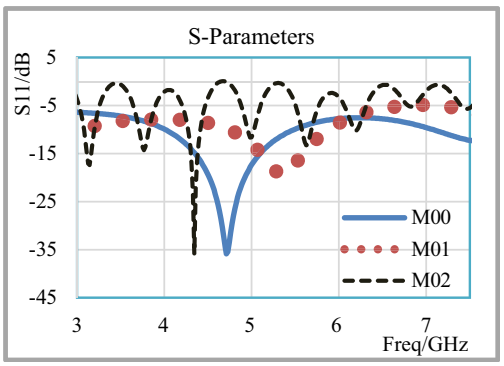

FIGURE 9. The S_{11} for the circular and annular patch when adding meta cell.

the values of the main targeted parameters for these models' bandwidth, gain, radiation efficiency, and return loss $|S_{11}|$ that are calculated in this work. Figure 10 shows a comparison according to the relationship between the frequency and return loss for these four models, and the figure also presents the effect of the proposed technique on the calculated parameters. In addition, it is necessary to note that the proposed design leads to reducing the size of the antenna to approximately half of the first model, then start to improve each of these models respectively and compare the calculated results to get the best model that is suitable to work at the target frequency in 6 GHz band, which is one of the frequency ranges for 5G WC.

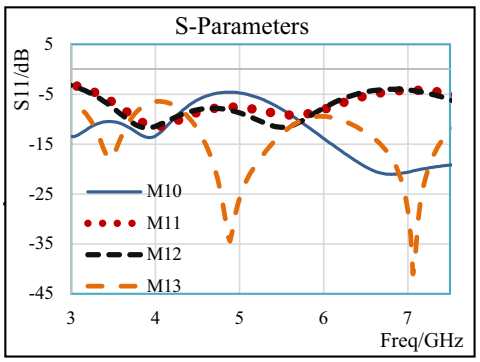

FIGURE 10. The S_{11} for the second group based on model M10.

The presented results in Table 9 represent the calculated parameters for the models M10, M12 and M13. The design of M13 improves these parameters in comparison with M10 that has a resonant frequency $f_r = 6.7051$, BW of 5.671–9.898 GHz, $S_{11} = -21.366$, gain (G) = 5.967, and radiation efficiency $\eta = 94.71$, while for M13 $f_r = 5.626$, $S_{11} = -39.034$, $G = 4.675$, $\eta = 92.89$, and BW of 4.997–6.594 via comparing Tables 8 and 9, the obtained results for the models M10, M11, M12, and M13 are better M00, M01, and M02 especially in the targeted band of the research topic 6 GHz.

However, with the use of the metasurface, each element of the second group of antennas will be studied respectively, which begins with M10 applying the metasurface technique. Figure 11 presents the relationship between the frequency and return loss for the three models of this group, and Table 10 shows the results of these models more clearly. The following tables display the effect of adding metasurface unit to the models on the parameters of antenna design proposed in this work, which were presented in the previous paragraph, where each table will work in an indirect way by displaying the results of comparing the model with itself first and with others secondly. The results presented in Table 10 shows the achievement of the new approach for the proposed design, which functions at the targeted frequency of 5G communications 6 GHz.

The meta technique leads to the decrease of resonant frequencies of the design with smaller dimensions and shows better return loss that relates to the matching impedance, good bandwidth, besides the excellent radiation efficiency and gain. Figure 11 shows the resonant frequency and reflection coefficient (or return loss $|S_{11}|$), in addition to the BW for M10. More-

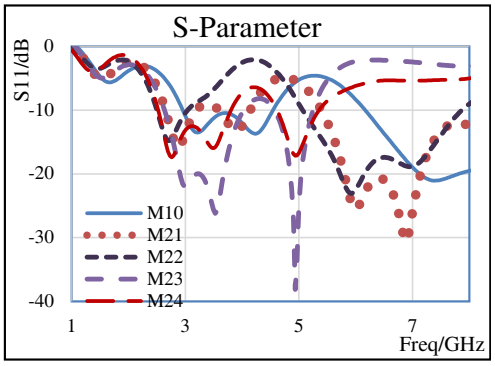

FIGURE 11. The effect of adding meta cell on the relation of (S_{11}) with frequency for M10.

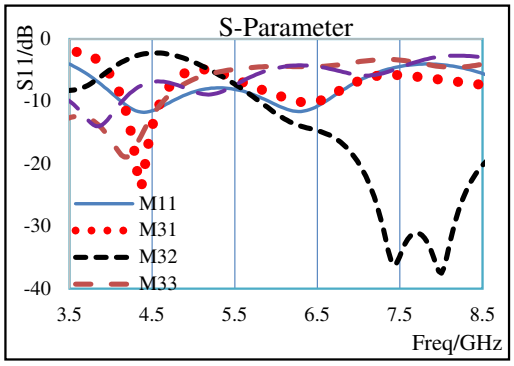

FIGURE 12. The effect of adding metasurface on the (S_{11}) for the model M11.

TABLE 10. The effect of adding meta cells on M10.

No	f_r GHz	S_{11} dB	BW GHz	G dBi	η %
M10	4.02	−12.87	1.57	3.45	96.9
	677	−21.3	4.32	5.9	94.7
M21	2.94	−14.5	0.70	3.02	98.7
	3.81	−14.8	05	3.39	98.1
	6.08	−26.80	4.4	5.28	93.2
M22	2.79	−13.0	0.6	2.8	99.1
	6.09 6	−21.6	2.9	5.3	94.1
	10.2	−22.37	1.37	6.02	86.4
M23	3.6	−33.2	1.5	3.25	97.1
	5.0	−11.90	0.4	4.3	89.6
M24	2.898	−15.25	1.5	2.8	97
	5.245	−18.02	0.85	5.08	92.8

over, it also presents the effect of adding meta cell to the proposed design of this model. The curves show the clear effect of meta cell on the antenna performance parameters. Figure 11 shows the best results obtained for the first model, the circular patch that resonates at the targeted frequency 6 GHz. Then at the third steps, according to Table 5, M10 = 6.771 GHz, M21 = 6.08 GHz, and M22 = 6.09 GHz.

The results in Table 11 are obtained by the simulation based on the models in Table 10 to display the results of model M11, where the same steps, following in the previous model, have been used. In the second model, which is the ring, considering the resonant frequencies, it is suitable for working in 5G communications networks that operate in a medium range of 6 GHz, as well as for the sixth generation communications that operate in a range from 7 to 20 gigahertz.

Figure 12 shows the results obtained for model M11 and calculated for the annular patch, which operates at the targeted frequency (6 GHz) and ordered according to their sequences in Table 11. For M32, $f_r = 7.941$, $G = 4.809$, and $\eta\% = 90.65$, but BW starts from 5.869 to 10.43 which means that the 6 GHz is already obtained in this band; the gain at 6 GHz is 4.758, $\eta\% = 90.68$; and return loss is $S_{11} = -38.707$. Comparing

TABLE 11. The effect of adding meta cells on M11.

No	f_r GHz	S_{11} dB	BW GHz	G dBi	η %
M11	2.7	−11.60	0.50	2.74	95.7
	8.30	−19.0	1.61	4.37	88.1
M31	2.80	−13.9	0.40	2.95	98.7
	4.35	−20.06	0.2	2.2	83.8
M32	2.768	−10.7	0.335	2.874	99.47
	7.941	−38.87	4.544	4.809	90.65
M33	3.755	−21.49	1.359	3.251	94.35
M34	2.911	−12.2	1.557	2.777	95.06

TABLE 12. The effect of adding meta cell on the parameters of M12.

No	f_r GHz	S_{11} dB	BW GHz	G dBi	η %
M12	6.0	−16.19	3.5	4.0	91.5
M41	2.78	−13.99	0.30	2.81	96.4
	4.32	−20.7	0.23	2.49	87.5
M42	7.22	−18.85	2.5	4.44	92.0
M43	3.74	−30.1	1.2	3.3	94.1
M44	3.4 9	−11.16	0.4	3.15	94.7
	4.0	13.01	0.5	3.56	93.7

the results of the two antennas (M10 and M11) in both Tables 10 and 11, they show excellent efficiency and have high gain, compared to that in Table 8.

The results illustrated in Table 12 present the effect of adding metasurfaces on the back side of the proposed antenna model M12. Figure 13 shows the effect of adding metasurface on the resonance frequency and BW via the relation between S_{11} and frequency. Table 13 shows the results obtained for M50 model at each resonant frequency. The table displays the main performance parameters, such as f_r, S_{11}, BW, G, and η. From Table 13 of model M13, which is similar to the previous models, the results contain multiple resonant frequencies.

In addition, the use of split ring resonant technique leads to a shift in the resonant frequencies, within the operating fre-

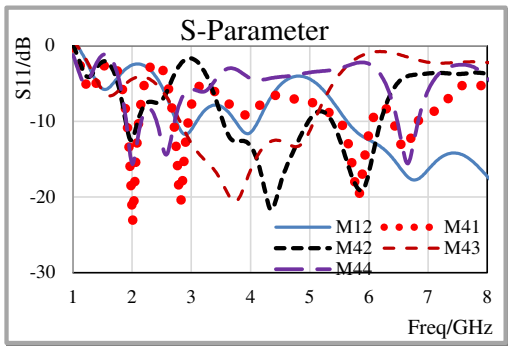

FIGURE 13. The effect of adding meta cells on the (S_{11}) for the model M12 .

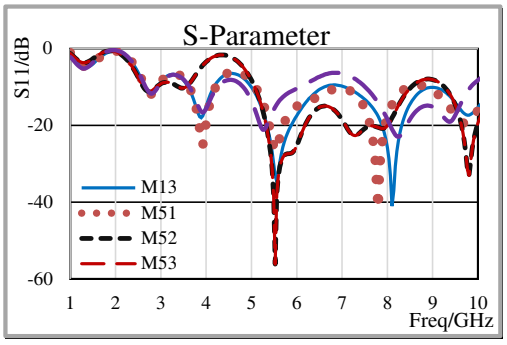

FIGURE 14. The effect on the (S_{11}) when adding metasurface to the model M13.

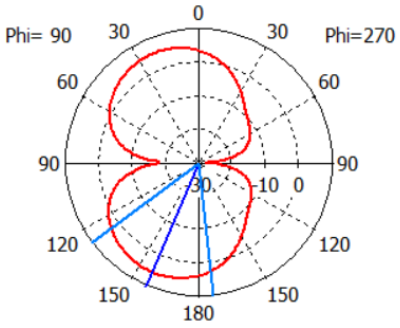

FIGURE 15. The radiation pattern of the circular patch antenna model M10.

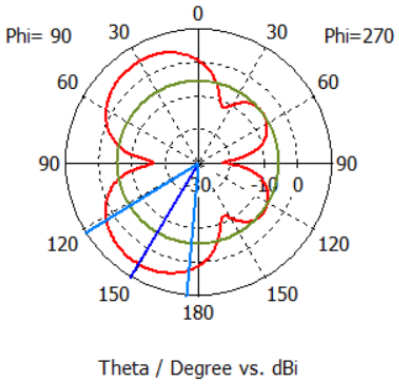

FIGURE 16. The radiation pattern of the circular patch antenna M32.

TABLE 13. The effect of adding meta cell on the parameters of M13.

No	f_r GHz	S_{11} dB	BW GHz	G dBi	η %
M13	3.9	−19.3	0.50	2.702	89.1
	5.6	−39.03	1.6	4.675	92.9
M51	4.03	−24.81	0.45	2.738	84.8
	5.5	−48.7	3.3	4.578	94.3
M52	5.69	−44.1	3.5	4.622	91.8
M53	4.0	−24.4	1.79	2.703	86.9
	5. 2	−13.9	1.2	4.201	88.5
M54	4.09	−19.5	0.5	2.971	89.2
	5.21	−27.35	1.2	3.745	90.39

quency range around 6 GHz, which is shown in Figure 14. From Table 13, all bands covering the 6 GHz frequency range have good readings for the target parameters shown in the table, with a gain value more than 3.5 dB and a radiation efficiency more than 90%. These common parameters of the four models, shown in tables and graphs, are suitable for 5G wireless communication applications due to their good results in terms of gain, bandwidth, return loss, and radiation efficiency.

Figures 15, 16, 17, and 18 illustrate show one-dimensional (1D) antenna radiation pattern of the four models M10, M32, M40, and M50 respectively at 6 GHz, which shows the width and direction of the radiation angle.

Figure 15 presents the 1D radiation pattern for the antenna model M10 at the frequency 6.2565 GHz, the direction of the main lobe at 157 degrees (DEG), and the angular beam width is 59.4 DEG. Figure 16 presents the 1D radiation pattern for the antenna model M32 at frequency 6 GHz, the direction of the main lobe at 149 DEG, and the angular beam width 53.42 DEG. Figure 17 presents the radiation pattern for antenna model M40 at 6 GHz frequency band, the main lobe direction at 156 DEG, and the angular beamwidth 67.6 DEG. Figure 18 presents the 1D radiation pattern for the antenna model M50 at frequency 6 GHz, the direction of the main lobe at 153 DEG, and the angular beam width 57.1 DEG. All in all, the calculated results illustrate an excellent improvement to the performance parameters of the circular patch microstrip antenna when the modern techniques are used like meta cells design (metamaterial).

The proposed design presents excellent results which make it suitable for the recent wireless communications (5G) including smartphones and other mobile devices, at the frequency range: C-band, 3.3–4.2 and 6 GHz, besides the other applications such as internet of things (IoT) and smart homes range of frequencies, 2.4–5 GHz. In addition, the frequency range of proposed model meets the requirements of vehicle to everything (V2X) communications, autonomous vehicles 5.9 GHz (V2X-specific bands), the frequency range for small cell, distributed antenna systems, robotics, and industrial automation range of frequencies: 2.4–6 GHz.

Table 14 presents a brief comparison to the calculated results for the proposed model with some of the previous literatures.

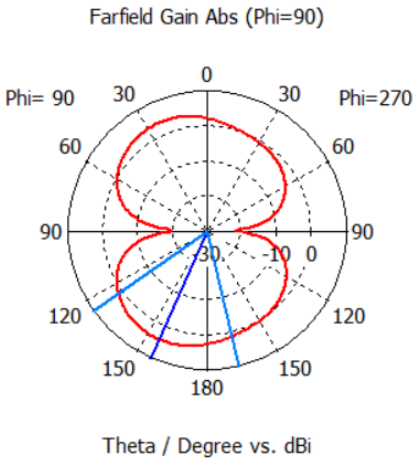

FIGURE 17. The radiation pattern of the circular patch antenna model M40.

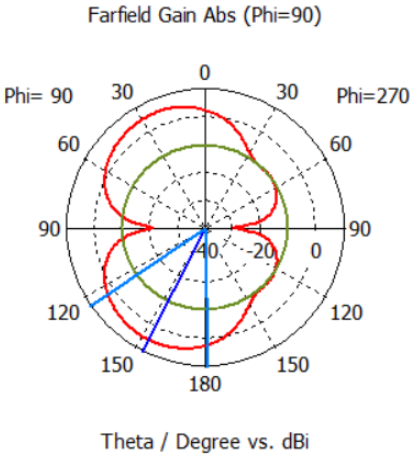

FIGURE 18. The radiation pattern of circular patch antenna model M50.

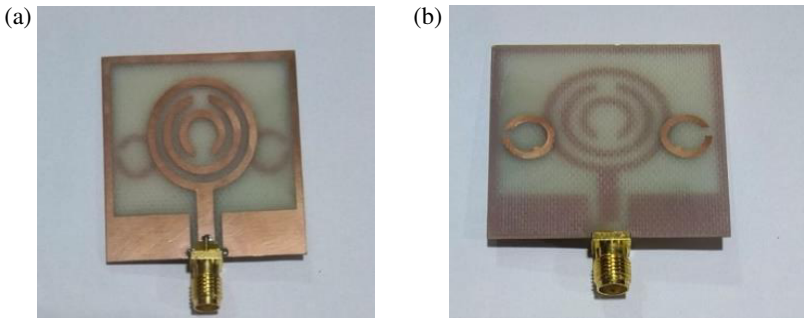

FIGURE 19. Experimental model. (a) Front side, (b) back side.

TABLE 14. The results comparison of the proposed antenna with the previous literatures.

Ref	Dim mm	f_r in GHz	BW in GHz	η in %	G in dBi
[21]	34 × 39	4.2	2.70	NR	2.25
[22]	60 × 60	2.24 3.66	0.29 0.34	NR	3.1 3.29
[23]	40 × 40	2.9 4.75	2.86 3.0	80	2.5 5.2
[12]	30 × 30	10.4	0.5		5.06
[24]	47 × 30	2.45 5.2	1.4 2	98.5 95.0	2.5 4.63
[25]	41 × 44	2.4 5.8	3.8 5.2	91.4 92.3	3.74 5.13
[26]	50 × 50	2.4 5.8	NR	16 25	1.69 4.12
[27]	100 × 100	2.4 5.8	4.9 3.8		1.90 5.90
Proposed	35 × 35	5.67	2.161	90.6	5.343

4. EXPERIMENT MANUFACTURING AND TESTING

In this part, the prototypes of the proposed model achieved the goal of this work. Model M52 was chosen from Table 13 for experimental testing. Firstly, during the design and simulation process, the model was implemented on an FR4 substrate with 1 mm thickness. After that at the time of fabrication process, the 1 mm substrate was not available in the lab, and a 0.8 mm substrate was available that can be used instead of the 1 mm substrate. Then, the design was changed to adapt with targeted band of frequencies. The use of a 0.8 mm substrate leads to decrease in thickness of the dielectric layer that means smaller size and less weight, which makes it more suitable for mobile devices. The meta cell (SRR) was used on the back layer layer, and some design changes were made, but it had less effect on the manufacturing model. Figure 19 shows the manufactured prototype. The fabricated model of the proposed antenna was tested via Agilent technologies vector network analyzer (VNA) model [E5017C]. Figure 20 shows the VNA, and Figure 21 shows the test results for the proposed model. After clarifying the difference in model M52 and modifying it for manufacturing, the selected model was validated via simulation of the proposed design using High Frequency Structure Simulator (HFSS) software. Then, the design was modified according to the manufacturing requirements.

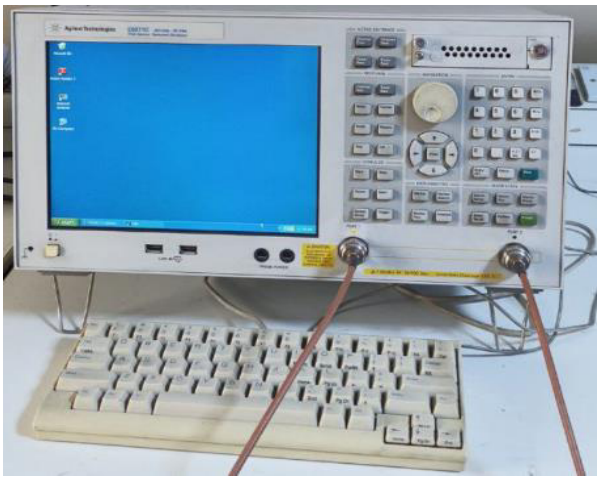

FIGURE 20. The Agilent VNA model [E5017C].

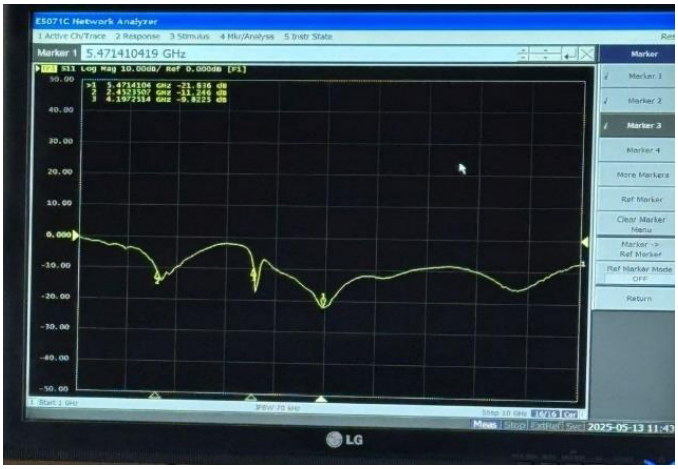

FIGURE 21. Photo to the display of the S_{11} result.

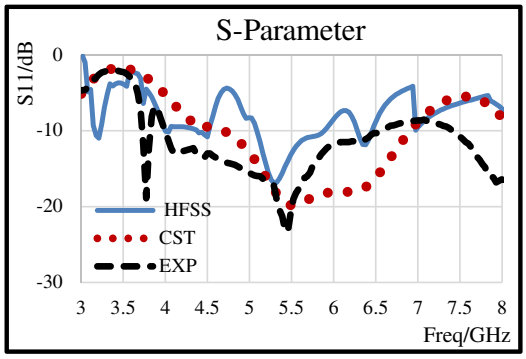

FIGURE 22. The calculated and measured (S_{11}) for the simulations and experimental model.

The results of the model for both environments, simulation and experiment, are shown in Table 15 and Figure 22. It is clear that both of them are multi-resonant, and their results are very close. It is also presented that the model is useful for operating in the frequency range from 4.5 to 7 GHz according to their S_{11}, bandwidth gain, and radiation efficiency.

5. CONCLUSIONS

This manuscript presents different techniques used in the improvement of circular patch antenna to make it suitable for 5G applications and operate around 6 GHz bands. The design has been developed from the traditional model, which has larger size and very narrow bandwidth, low gain, and radiation efficiency for the antenna that operates in the band of 5G at 6 GHz frequency. The new design is around half size of the traditional circular patch, has larger bandwidth, high gain, and radiation efficiency of approximately over 90%. In short, the use of meta technique improves the antenna design, which makes it efficient to be used for 5G applications based on the selected proposed model that shows an excellent matching between theoretical and experimental results.

TABLE 15. The simulated and experimental results.

No	f_r GHz	S_{11} dB	BW GHz	G dBi	η %
exp	5.5	−21.8	2.287	/	/
CST Sim	5.67	−22.07	2.192	5.343	90.59
HFSS Sim	5.29	−17.2	0.82	5.128	94.49

ACKNOWLEDGEMENT

The manuscript has been done with the support of the Department of Electrical Engineering at the University of Babylon. The sample of the proposed model had been tested in the Department of Electronic and Communication at Al Nahrain University.

REFERENCES

[1] Wang, Y., L. Sun, Z. Du, and Z. Zhang, "Review antenna design for modern mobile phones: A review," *Electromagnetic Science*, Vol. 2, No. 2, 1–36, 2024.

[2] Lashab, M., M. Belattar, S. Hocine, and H. Ahmed, *Metamaterial Applications in Modern Antennas*, 1–18, IntechOpen, 2022.

[3] Younus, S. Y. and M. T. Gatte, "Design of dual bands microstrip patch antenna for 5G applications," in *AIP Conference Proceedings*, Vol. 2804, No. 1, 020030, Baghdad, lraq, 2023.

[4] Kadhim, R. A., Y. N. Jurn, and M. T. Gatte, "Dual band antenna in licensed and unlicensed frequency bands based on superformula for 5G applications," *Bulletin of Electrical Engineering and Informatics*, Vol. 12, No. 5, 2846–2851, 2023.

[5] Huang, Y., N. Khiabani, Y. Shen, and D. Li, "Terahertz photoconductive antenna efficiency," in *2011 International Workshop on Antenna Technology (iWAT)*, 152–156, Hong Kong, China, 2011.

[6] Gatte, M. T., P. J. Soh, H. A. Rahim, R. B. Ahmad, and F. Malek, "The performance improvement of THz antenna via modeling and characterization of doped graphene," *Progress In Electromagnetics Research M*, Vol. 49, 21–31, 2016.

[7] Gatte, M. T., P. J. Soh, H. A. Rahim, R. B. Ahmed, and F. Malek, "Improvement of a millimeter-wave hexagonal patch antenna using doped graphene," *Advanced Science Letters*, Vol. 23, No. 6,

5342–5345, 2017.

[8] Gatte, M. T., P. J. Soh, R. A. Kadhim, H. J. Abd, and R. B. Ahmad, "Modeling and performance evaluation of antennas coated using monolayer graphene in the millimeter and sub-millimeter wave bands," *International Journal of Numerical Modelling: Electronic Networks, Devices and Fields*, Vol. 34, No. 5, e2929, 2021.

[9] Gatte, M. T., P. J. Soh, M. F. Jamlos, R. B. Ahmad, M. F. Malek, and H. A. Rahim, "Improvement of metal-based THz patch antenna parameters using monolayer graphene," in *The 7th International Conference on Metamaterials, Photonic Crystals and Plasmonics, META'16 Malaga — Spain*, 1716–1720, Torremolinos (Malaga), Spain, 2016.

[10] Tadesse, A. D., O. P. Acharya, and S. Sahu, "Application of metamaterials for performance enhancement of planar antennas: A review," *International Journal of RF and Microwave Computer-Aided Engineering*, Vol. 30, No. 5, e22154, 2020.

[11] Karimbu Vallappil, A., M. K. A. Rahim, B. A. Khawaja, and M. N. Iqbal, "A miniaturized metamaterial-loaded switched-beam antenna array system with enhanced bandwidth for 5G applications," *IEEE Access*, Vol. 12, No. 6684-6697, 2024.

[12] Kamil, A. Q., H. M. Kadhim, and R. M. Alsammarraie, "Gain improvement for single band ultra-wideband antenna by slots technique," in *2024 21st International Multi-Conference on Systems, Signals & Devices (SSD)*, 755–760, Erbil, Iraq, 2024.

[13] Chomtong, P., P. Krachodnok, J. Konpang, N. Somjit, C. Mahatthanajatuphat, and P. Akkaraekthalin, "Miniaturized multiband EBG reflector using DICPW structure for wireless communication systems," *IEEE Access*, Vol. 12, 30 398–30 415, 2024.

[14] Sable, S. K., R. Mishra, and S. R. Nigam, "Characteristics enhancement of microstrip patch antenna by using metamaterial rings," *Far East Journal of Electronics and Communications*, Vol. 18, No. 5, 723–736, 2018.

[15] Khan, D., A. Ahmad, and D.-Y. Choi, "Dual-band 5G MIMO antenna with enhanced coupling reduction using metamaterials," *Scientific Reports*, Vol. 14, No. 1, 96, 2024.

[16] Godaymi Al-Tumah, W. A., R. M. Shaaban, and A. P. Duffy, "Design, simulation, and fabrication of a double annular ring microstrip antenna based on gaps with multiband feature," *Engineering Science and Technology, An International Journal*, Vol. 29, 101033, 2022.

[17] Hashim, R. M. and M. T. Gatte, "Employment of meta technologies for efficient design of a planner antenna at 5G frequency bands," in *2024 3rd International Conference on Advances in Engineering Science and Technology (AEST)*, 138–141, Babil, Iraq, 2024.

[18] Bhobe, A. U., C. L. Holloway, M. Piket-May, and R. Hall, "Wide-band slot antennas with CPW feed lines: Hybrid and log-periodic designs," *IEEE Transactions on Antennas and Propagation*, Vol. 52, No. 10, 2545–2554, 2004.

[19] Li, K., C. H. Cheng, T. Matsui, and M. Izutsu, "Study on coplanar fed CPW patch antennas," in *Proceedings of the International Symposium on Antennas and Propagation Japan*, Vol. 3, 1111–1114, Fukuoka, Japan, 2000.

[20] Colaco, J. and R. Lohani, "Design and implementation of microstrip circular patch antenna for 5G applications," in *2020 International Conference on Electrical, Communication, and Computer Engineering (ICECCE)*, 1–4, Istanbul, Turkey, Jun. 2020.

[21] Jangid, K. G., V. S. Kulhar, V. Sharma, A. Tiwari, B. Sharma, and D. Bhatnagar, "Compact circular microstrip patch antenna with modified ground plane for broadband performance," in *2014 International Conference on Signal Propagation and Computer Technology (ICSPCT 2014)*, 25–28, Ajmer, India, Jul. 2014.

[22] Rajanna, V. K. S., T. Venkatesh, P. K. T. Rajanna, and M. Shambulinga, "A triband slot antenna loaded with asymmetric split ring resonator for wireless applications," *Progress In Electromagnetics Research Letters*, Vol. 117, 61–67, 2024.

[23] Ohi, M. A. R., Z. Hasan, S. F. B. Faruquee, A. A. M. Kawsar, and A. Ahmed, "Wideband Minkowski fractal antenna using complementary split ring resonator in modified ground plane for 5G wireless communications," *Engineering Reports*, Vol. 3, No. 9, e12388, 2021.

[24] Khan, M. A., W. T. Sethi, W. A. Malik, A. Jabbar, M. A. Khalid, A. M. Almuhlafi, and M. Himdi, "A comprehensive analysis of low-profile dual band flexible omnidirectional wearable antenna for WBAN applications," *IEEE Access*, Vol. 12, 45 187–45 201, Mar. 2024.

[25] Musa, U., S. M. Shah, H. A. Majid, I. A. Mahadi, M. K. A. Rahim, M. S. Yahya, and Z. Z. Abidin, "Design and analysis of a compact dual-band wearable antenna for WBAN applications," *IEEE Access*, Vol. 11, 30 996–31 009, Mar. 2023.

[26] Bhattacharjee, S., S. Maity, S. R. B. Chaudhuri, and M. Mitra, "A compact dual-band dual-polarized omnidirectional antenna for on-body applications," *IEEE Transactions on Antennas and Propagation*, Vol. 67, No. 8, 5044–5053, 2019.

[27] Zhou, L., S. Fang, and X. Jia, "Dual-band and dual-polarised circular patch textile antenna for on-/off-body WBAN applications," *IET Microwaves, Antennas & Propagation*, Vol. 14, No. 7, 643–648, 2020.